Grasp-State Plane Analysis of Two-Phalanx Underactuated Fingers

Lionel Birglen *,

Department of Mechanical Engineering, Ecole Polytechnique, Montréal, QC, H3T 1J4, Canada

Clément M. Gosselin

Department of Mechanical Engineering, Laval University, Québec, QC, G1K 7P4, Canada

Abstract

This paper presents a new technique to analyze the grasp stability of two-phalanx underactuated fingers of general architecture using a grasp-state plane approach. Similarly to the state plane analysis for dynamical systems, a grasp-state plane technique is very elegant and efficient to study the grasp stability of two-phalanx underactuated fingers. The concept of underactuation in robotic fingers—with fewer actuators than degrees of freedom—allows the hand to adjust itself to an irregularly shaped object without complex control strategy and numerous sensors. However, in some configurations, the force distribution of an underactuated finger can degenerate, i.e. the finger can no longer apply forces on the object. This situation leads in some cases to the ejection of the object from the hand. This paper focuses on two-phalanx fingers and studies their ability to seize objects with a secure grasp, considering practical issues on the grasp, namely the local geometry of the contact, the influence of design parameters and friction. A grasp-state representation which allows to accurately visualize the contact state trajectory as well as equilibrium and unstable situations is presented.

Key words: robot hand, underactuated fingers, stable grasp, shape adaptation, grasp-state.

* Corresponding author.
Email addresses: lionel.birglen@polymtl.ca (Lionel Birglen), gosselin@gmc.ulaval.ca (Clément M. Gosselin).

1 Introduction

Until now, the human hand remains unmatched despite numerous and interesting attempts. Pioneer designs include: the Utah/MIT hand [1], the Stanford/JPL (Salisbury's) hand [2], the Belgrade/USC hand [3], the Barrett-Hand [4], the hands from the DLR [5], the Okada hand [6], and many others. However, significant efforts have been made to find designs that are simple enough to be easily built and controlled in order to obtain practical systems [7], particularly in human prosthetics. The lack of success of these complex devices is mainly due to the cost of the control architecture needed with often more than ten actuators plus many sensors. In order to overcome these limitations, a particular emphasis has been placed on the reduction of the number of degrees of freedom, thereby decreasing the number of actuators. On the other hand, very few prototypes involve a smaller number of actuators without decreasing the number of degrees of freedom. This approach, referred to as *underactuation* can be implemented through the use of passive elements like mechanical limits or springs leading to a mechanical adaptation of the finger to the shape of the object to be grasped [8,9,10,11,12]. The idea to approach the spatial complement of the shape of an object to ensure a distributed grasp is rather common in biologically-inspired robotics: e.g. snake robots or elephant trunks. They belong to what has been defined as the Frenet-Serret manipulators [13] intended for whole-arm manipulation [14]. General grasping processes have also been discussed in [15]. The present analysis stems from results introduced in [16] and is based on an approach proposed in [17]. In this paper, the authors present the grasp analysis of a complex and refined model of two-phalanx underactuated finger, considering friction, the influence of springs, an arbitrary local shape of the contact and any kind of mechanical architecture. Examples are given considering four-bar linkage and pulley-tendon transmissions but the results can be easily extended to any type of mechanism (gears, multiple pulley wiring, etc.).

2 Force Properties of Underactuated Fingers

Underactuation in robotic fingers is different from the concept of underactuation usually presented in robotic systems and both notions should not be confused. An underactuated robot is generally defined as a manipulator with one or more unactuated joints. On the other hand, underactuated fingers generally use elastic elements in their "unactuated" joints. Thus, one should rather think of these joints as *uncontrollable* or *passively driven* instead of unactuated. In an underactuated finger, the actuation wrench T_a is applied to the input of the finger and is transmitted to the phalanges through suitable mechanical elements, e.g. four-bar linkages, pulleys and tendons, gears,

etc. Since underactuated fingers have many degrees of freedom, and fewer actuators, passive elements are used to kinematically constrain the finger and ensure the shape-adaptation of the finger to the object grasped. To this end, springs and mechanical limits are often used. An example of underactuated two-phalanx finger using linkages and its closing sequence are illustrated in Fig. 1. The actuation torque T_a is applied to the first link which transmits the effort to all phalanges. Notice the mechanical limit that allows a pre-loading of the spring to prevent any undesirable motion of the second phalanx and also to prevent hyperextension of the finger. Springs are useful for keeping the finger from incoherent motion, but when the grasp sequence is complete, they still oppose the actuation. Thus, springs shall be designed with the smallest stiffness possible, however sufficient to keep the finger from collapsing. With practical prototypes, one has to ensure that grasps are stable in the sense that ejection is prevented. Indeed, an ideal grasping sequence as illustrated in Fig. 1 does not always occur. For in the final configuration some phalanx forces may be negative. If one phalanx force is negative the corresponding phalanx will loose contact with the object. Then, another step in the grasping process will take place: the remaining phalanges corresponding to positive forces will slide on the object surface. This sliding process will continue until either a stable configuration is achieved, or the last phalanx will curl away and loose contact with the object (ejection, Fig. 2).

3 Introducing the Grasp-State Plane

3.1 Single Point Contact

Note that in this work, a stable grasp means that the finger is in static equilibrium. Contrary to the usual concept of "stability" used in grasping analysis, a stable grasp will hereinafter designate a grasp situation where all phalanx forces are positive or zero. This is different from force- or form-closure and is a necessary condition to be achieved to ensure one or the other previous forms of stability. A model for the fingers under study is presented in Figs. 3-4. The contact force expressions have been established in [17]:

$$\mathbf{f} = \mathbf{J}^{-T}\mathbf{T}^{-T}\mathbf{t} \tag{1}$$

where $\mathbf{f}^T = [f_1,\ f_2]^T$ is the vector of the contact force expressions, $\mathbf{t}^T = [T_a,\ T_2]^T$ is the input torque vector exerted by the actuator (T_a) and the spring between the phalanges (T_2). The matrix $\mathbf{J}$ is the Jacobian matrix of the grasp (which may include friction [18] or not [17]) and $\mathbf{T}$ is the transmission matrix characterizing the underactuation mechanism used to transmit the

motion [17], i.e.

$$\mathbf{J}=\begin{bmatrix} k_1 & 0 \\ k_2+l_1(\cos\theta_2+\mu\sin\theta_2) & k_2 \end{bmatrix} \text{ and } \mathbf{T}=\begin{bmatrix} 1 & R \\ 0 & 1 \end{bmatrix}. \tag{2}$$

where μ relates the tangential contact force f_{t2} to the normal contact force f_2, i.e $f_{t2}=\mu f_2$. This coefficient is usually unknown, but has on the edge of the friction cone (and only on the edge of the friction cone) a particular value, namely the static friction coefficient $\mu=\pm\mu_{static}$.

For instance and initially without friction, i.e. $\mu=0$, for a mechanically-driven finger (Fig. 4), one has $R=-h/(h+l_1)$ [17], hence:

$$\mathbf{f}=\begin{bmatrix} -\frac{l_1(-k_2+h\cos\theta_2)}{k_1k_2(h+l_1)}T_a-\frac{k_2+l_1\cos\theta_2}{k_1k_2}T_2 \\ \frac{h}{k_2(h+l_1)}T_a+\frac{1}{k_2}T_2 \end{bmatrix}, \tag{3}$$

where h is the directed distance between point O_1 and the geometric intersection of lines (OO_1) and (P_1P_2) (this distance can be negative).

For tendon-actuated fingers (Fig. 4), $R=-\alpha=-r_2/r_1$ and

$$\mathbf{f}=\begin{bmatrix} -\frac{-k_2+\alpha k_2+\alpha l_1\cos\theta_2}{k_1k_2}T_a-\frac{k_2+l_1\cos\theta_2}{k_1k_2}T_2 \\ \frac{\alpha}{k_2}T_a+\frac{T_2}{k_2} \end{bmatrix} \tag{4}$$

with $T_a=F_a/r_1$.

Then, one can study the condition under which both f_1 and f_2 are positive (or not), which depends on the contact situation, namely the pair (k_2,θ_2), but neither on θ_1 nor on k_1. This pair defines a plane, where the contact situation can be tracked. This plane will be referred to as the grasp-state plane. An example of configurations with fully positive contact forces is presented in Fig. 5 for a set of geometric parameters presented in Table 1. Shaded areas are unstable contact configurations where

$$f_1<0 \quad \text{or} \quad f_2<0 \tag{5}$$

It should be emphasized that, with a fully actuated finger, the stable zones will cover the whole plane. Conversely, in Fig. 5, a not so particular example, situations with both positive phalanx forces are minority cases.

When in an unstable configuration (one of the phalanx force is negative), the closing process will force the finger to lose contact with the phalanx with a negative force, usually the proximal one. Then, contact will only remain with

Table 1
Geometric parameters

Set	l_1	l_2	ψ	a	b	c
1	1	2/3	90°	1	1	1/3
2	1	2/3	90°	2/3	1	1/3
Soft Gripper	1	1	–	1	–	1/3

the distal phalanx, and the finger will slide against the object. If $f_1 < 0$, an equilibrium position can still be attained but just for a one and unique particular position of contact k_2. This is, of course, the position corresponding to the solution of the equation $f_1(k_2) = 0$, i.e.

$$k_2 = e = -\frac{R}{1+R} l_1(\cos\theta_2 + \mu \sin\theta_2) \tag{6}$$

if the spring is neglected. In the case of mechanically-driven fingers, one obtains

$$e = h(\cos\theta_2 + \mu \sin\theta_2). \tag{7}$$

Physically, eq. (7) implies that the contact force should be located on the projection onto the distal phalanx of the intersection of lines (OO_1) and (P_1P_2). Indeed, the distal phalanx is subjected to three pure forces, thus equilibrium can only exist if they all intersect in a common point. However this geometric interpretation no longer holds if the spring is taken into account. For tendon-driven fingers, one has:

$$e = \frac{r_2}{r_1 - r_2} l_1(\cos\theta_2 + \mu \sin\theta_2). \tag{8}$$

It should be noted that the distal phalanx force is always positive with tendon-driven finger, whereas in hyperflexion/hyperextension configurations with mechanical transmissions (illustrated in Fig. 6), this distal force can become negative. The hyperflexion/hyperextension configurations are delimited by the horizontal lines at approx. $\theta_2 = -45°$ and $\theta_2 = 160°$ in Fig 5 for that particular parameter set and are responsible for most of the large unstable areas in the latter figure, the others corresponding to a contact below the equilibrium point where $f_1 < 0$. However, it should be noted that such configurations with large values of θ_2 are usually not achievable with both kinds of transmission due to mechanical limits, common limits on θ_2 being $0 < \theta_2 < \pi/2$.

3.2 On the Grasp-State Plane Necessity

The next natural step is to determine if a design could be found that always avoids the loss of contact with one phalanx, i.e. a finger where both f_1 and f_2

are always positive. One may consider a general underactuated finger design characterized by its transmission matrix $\mathbf{T}$:

$$\mathbf{T} = \begin{bmatrix} 1 & R(\theta_2) \\ 0 & 1 \end{bmatrix}, \tag{9}$$

where R is the transmission factor. If the spring and friction are neglected, one obtains the analytical expression of the contact forces from eq. (1):

$$\mathbf{f} = \begin{bmatrix} \frac{k_2(1+R)+Rl_1\cos\theta_2}{k_1k_2}T_a \\ -\frac{R}{k_2}T_a \end{bmatrix} \tag{10}$$

Assuming that $k_1 > 0$, $k_2 > 0$ and $T_a > 0$, to ensure that both elements are positive, one has:

$$R(\theta_2) < 0, \quad \forall\theta_2 \tag{11}$$

from the definition of f_2, and from the definition of f_1:

$$k_2\left(1 + R(\theta_2)\right) + R(\theta_2)l_1\cos\theta_2 > 0. \tag{12}$$

Therefore

$$\begin{cases} R(\theta_2) > \frac{-k_2}{k_2+l_1\cos\theta_2} & \text{if } k_2 + l_1\cos\theta_2 > 0 \\ R(\theta_2) < \frac{-k_2}{k_2+l_1\cos\theta_2} & \text{otherwise} \end{cases} \tag{13}$$

For $-\pi/2 < \theta_2 < \pi/2$, one obtains $R(\theta_2) > \frac{-k_2}{k_2+l_1\cos\theta_2}$ for any k_2. The limit case $k_2 = 0$ yields to $R(\theta_2) > 0$, this is in contradiction with eq. (11) and therefore $R(\theta_2)$ such that f_1 and f_2 are positive (for all possible values of k_2) does not exist at least for this range of angle θ_2. Indeed, only the function $R(\theta_2) = 0$ satisfies the positiveness condition on f_1 and f_2, however not stricly since in this case $f_2 = 0$ for any value of angle θ_2. This paradox can be graphically illustrated using Fig. 5: the stable fully positive contact configuration are located on top of the equilibrium curve. If these stable areas are to correspond to the whole range of the contact location k_2, the only possibility is an equilibrium value that is always zero. Since the latter is proportional to the coefficient R (see eq. 6), one obtains that R must also be zero. This proves that there is no design of underactuated finger that can provide a fully positive workspace, neglecting spring and friction for all possible contact locations. Therefore one **must** study the grasp-state plane in case of a single contact to prevent ejection.

4 Grasp-state Plane, Revisited

4.1 Contact Trajectories

If proximal contact is lost, one has to establish the behaviour of the finger to determine if a stable position will be reached or not. To obtain this evolution, the contact location as seen from the distal phalanx will be introduced. It can be easily shown by considering the triangle constituted by O_1, O_2 and the contact point (illustrated in Fig. 7), that if only this contact exists and if it is fixed in space, one has

$$k_2^2 - k_{2i}^2 + 2l_1(k_2 \cos\theta_2 - k_{2i} \cos\theta_{2i}) = 0 \tag{14}$$

where k_{2i} and θ_{2i} are an arbitrary initial configuration, for example, the precise instant when the contact on the first phalanx is lost. This equation expresses that the distance between the base point of the finger and the contact location is constant for any pair (k_2, θ_2). Eq. (14) is actually a hyperbola in the plane $(k_2,\cos\theta_2)$ centred in $(0, 0)$. The contact hyperbola corresponds to a complex curve in the plane (k_2,θ_2) which is actually similar to an hyperbola. The contact curves in the (k_2,θ_2) plane are illustrated in Fig. 8.

Eq. (14) allows to obtain the evolution of the contact position with respect to the evolution of θ_2. In these situations, the finger now has one degree of freedom while keeping contact with the object, this motion has been previously noticed and referred to as self-posture changing motion [19]. The contact situation evolves on the contact trajectory defined by eq. (14) and also by its relative location with respect to the equilibrium position, which indicate the sign of f_1. Indeed, the contact trajectory is a curve in the contact plane (k_2, θ_2), so the direction in which the contact situation travels on that curve, choosing from the two possible directions, is not immediate but can determined by studying the sign of f_1. For instance, in the central part of the contact trajectories (where there is an intersection with the horizontal line $\theta_2 = 0$), if the contact location is located below the equilibrium point, the finger undergoes an opening motion and θ_2 decreases. The contact evolution is indicated by arrows in Fig. 9 to illustrate this point. The contact state, defined by the pair (θ_2, k_2), evolves along the trajectories defined by eq. (14), and then, if the contact trajectory crosses the equilibrium equation defined by eq. (6), the grasp is finally stable, or else contact with the object will be lost, namely one obtains the ejection phenomenon either due to the kinematic evolution ($k_2 \geq l_2$, illustrated in Fig. 2), or due to the hyperflexion/hyperextension configurations. Depending on the geometric parameters (Table 1) of the mechanism, one can draw the final stability of the grasp depending on the initial contact situation, examples are presented Figs. 9, 10, and 11.

The contact trajectories defined above are indicated by dotted lines in the latter Figures, the arrows indicate the direction of the contact evolution, and the blue solid lines indicate the equilibrium equation (labeled "repulsive" and "attractive" frontier). However, if conclusions on the final stability of the grasp can be drawn from this plane, any notion of time is missing from the analysis. If the contact situation corresponds to a stable final grasp, this grasp will be achieved, however, the time required to achieve this equilibrium situation is totally unknown and depends on the dynamics of the system. The three steps necessary to construct the stability areas of the grasp-state plane are illustrated in Fig. 12. First, the equilibrium equation and the contact trajectories (with the direction of the contact state evolution) are plotted. Second, the mechanical limits on the joint rotation are added with the unstable curve(s) corresponding to the loss of the distal contact. The ejection limit is the rightmost edge of the plane. Finally, the stability regions can be constructed by inspecting if an arbitrary initial grasp-state will lead to a stable situation (equilibrium curve or mechanical limit) or not.

Given the evolution of θ_2, one can separate the equilibrium curve in two distinct stable parts, one attracting limit (the lower part on the graph) and a repulsive limit (upper part), the transition between the two modes being the tangent point between the contact trajectories and the equilibrium curve. This point is labeled "paradox point" (Fig. 9) since it belongs to both the attractive and the repulsive frontier. When the equilibrium point physically leaves the phalanx, i.e. $\exists\theta_2 \mid e(\theta_2) > l_2$, another unstable frontier appears, e.g. in Fig. 10. The contact situations under the equilibrium curve and on the right hand side of the stability limit (shaded area number 2) are unstable because the contact trajectories cross the boundary $k_2/l_2 = 1$ before attaining the attractive equilibrium limit. The latter is not physically on the phalanx for this trajectory and this parameter set. This corresponds to the ejection phenomenon depicted in Fig. 2, ejection for a closing motion (θ_2 increases) of the distal phalanx. Ejection for an opening motion (θ_2 decreases) of the distal phalanx can also occur (shaded area number (1) in Fig. 10). In Fig. 9 it was the only form of ejection possible for common ranges of angle θ_2. If the distal phalanx tends to open, the motion of link a (and thus, the motion as seen from the actuator) is however still a closing process. Nevertheless, the contact situation will open the finger.

The large regions of instability in Fig. 5 should also be moderated, because one should remember that unstable regions in this figure (other than hyperflexion/hyperextension configurations) are caused by a contact situation under the equilibrium curve, which correspond to stable one-phalanx contact grasps. Each stability region is, in the usual range of motion, dual to the other, at least between these hyperflexion/hyperextension configurations. Hence, in most cases, i.e. when the contact is initially established with the proximal pha-

lanx, the final grasp will be stable with the notable exception of the second type of unstable region illustrated in Fig. 10. This type of instability should therefore be avoided as much as possible through suitable design. In conclusion, the equation of the equilibrium curve is of the uttermost importance for the stability of the grasp. One shall then proceed with some details of this function.

4.2 Equilibrium Point Equation

4.2.1 Spring issues

The equilibrium locus, defined in eq. (6), is primarily function of the ratio R as established in [16]. However some parameters neglected in [16] can have a significant contribution to the overall stability of the finger. For instance, if the spring is not neglected, deviations of the equilibrium curve are observed depending on the ratio between the input torque and the spring torque, note that for the usual range of motion of θ_2 ($0 < \theta_2 < \pi/2$), the spring tends to move the equilibrium locus closer to the base of the distal phalanx. This behaviour tends to eliminate the closing-ejection presented in the previous section and therefore the spring, has for this range of motion, a stabilizing effect on the system. This only corresponds to a local behaviour over the usual range of motion of the second phalanx and with moderate spring stiffness. Indeed, if the spring is too stiff, the grasp can degenerate for certain positions, with an equilibrium point pushed to infinity. If

$$\frac{T_2}{T_a} = 1 + R, \tag{15}$$

then the equilibrium location is not attainable, i.e. $e = \infty$. Eq. (15) will be referred to as the spring-degeneracy condition and it allows to obtain the finger configuration, characterized by the angle θ_2, corresponding to an impossible equilibrium. This degeneracy condition depends on the spring stiffness and central position. Furthermore, it also depends on the transmission index which can be a function of the geometric configuration of the finger. One can obtain a condition for non-degeneration, namely that the solution of eq. (15) for θ_2 corresponds to an angle that is not physically possible to achieve.

4.2.2 Friction

If friction is also considered during the grasp, eq. (6) is used to obtain the equilibrium locus. However, there is no longer a single equilibrium curve but rather two curves. The sign of μ defines these two curves in the grasp-state plane, each corresponding to one sliding direction, i.e. $\mu = +\mu_{static}$ or $\mu = -\mu_{static}$.

These curves are not *really* equilibrium curves as previously discussed, for they do not correspond to situations where $f_1 = 0$ but they characterize the sliding resistance due to the friction. The area between these two curves described by $\mu = \pm\mu_{static}$ correspond to a value of the coefficient μ such that $-\mu_{static} < \mu < +\mu_{static}$. In this case, recalling the definition of this coefficient, the tangential force on the phalanx is within the static friction cone. Therefore, since a rolling motion of the phalanx around the contact point is kinematically not feasible (except infinitesimally when $\theta_2 = 0$), the second phalanx is stuck and the finger will not slide anymore. Finally, the grasp is stable again, this time with $f_1 \neq 0$ but this non-zero normal force simply compensates the tangential distal phalanx force in order to achieve the overall static equilibrium of the finger.

The coefficient of friction depends on the material of the object-finger surface pair, numerical values [1] are $1 - 4$ for solid-rubber (idem). This is interesting since a robotic finger surface is usually covered with rubber to increase friction or indirectly by using a tactile sensing device. A graphical illustration in the case of rubber contact (a conservative value of 2 has been chosen) is presented in Fig. 13. The grey shaded areas correspond to a tangential distal force inside the friction cone, leading to a stable grasp.

4.3 Linear and Circular Contact

If the contact geometry is no longer a single point, the results of the preceding section do not hold true because the contact trajectories are no longer valid. Indeed, the contact trajectories allowed to establish a relationship between the two state variables of the grasp, namely k_2 and θ_2. This relationship depends on the local geometry of the object being seized. To be complete, a more general case should be studied, namely a contact with a local curvature. The two extreme cases of a curvature being the line, i.e. an infinite radius curvature, and the single point—the previously studied case—accounting for a zero radius curvature.

4.3.1 Linear contact

First let us consider the linear contact, the mobility of the finger with a distal linear contact is 0 except in particular configurations where $\theta_2 = \pm\pi/2$. Even in these particular cases, the mobility is only locally increased to 1. Thus, if a linear contact is established and maintained, the finger can be assumed to be in equilibrium. One can relate the linear contact with the previous section by

[1] from *The Machinery's Handbook 23, Industrial Press Inc.*

considering the two extremities or vertices of this line segment. Consider a linear contact, made by an arbitrary closing sequence: if this contact is unstable, contact will be lost with the line but not with the vertices (the contact force is assumed to be positive). Therefore, the final grasp will be stable if the sliding motion of the phalanx converges toward an equilibrium position as previously discussed or if the motion corresponding to the contact on each one of the two vertices of the line segment tend to bring the phalanx back in contact with the line. The latter case is indeed a stable linear contact while the other guarantees a stable grasp but only with a contact on one vertex. Since studying the behaviour of the finger with respect to the vertices of the line segment is sufficient to discuss the stability issue, one can use the grasp-state plane introduced above and the associated contact trajectories. The representation of a linear contact in this plane is simply a line segment with a length corresponding to the ratio of its physical length with the distal phalanx length. Example of linear contacts are presented in Fig. 14, the Cartesian line segments correspond to horizontal bold red lines in the grasp-state plane.

Therefore, one obtains two contact trajectories, each corresponding to one vertex of the line. If both vertices belong to stable contact trajectories, the grasp will be stable. If both vertices belong to unstable contact trajectories, the finger will lose the object. The latter holds even if the equilibrium curve is intersected since any deviation around this situation will induce a motion that leads to ejection. However, if one contact trajectory is stable and the other leads to ejection, the case must be investigated. To ensure a stable linear grasp, the single force equivalent to the distributed load acting on the phalanx by the line, which is at the centroid of this load, must be located on an equilibrium position. However, this load distribution is not know and is not necessarily a hyperbolic function of the contact location k_2 as the contact force in eq. (1). If the initial contact with the line is made with a vertex whose contact trajectory corresponds to a certain evolution of θ_2 and the second contact with a vertex corresponding to an opposite evolution of θ_2 then the linear grasp is stable. The stability of the initial linear contact is illustrated in Fig.17. Inspection of Figs. 9–11 reveals that, two different cases should be considered, depending on the quadrant in which the hyperbolic trajectories the contact situation is located:

- if the latter is between the two asymptotes (central part of the figures), this change of direction can only happen if each contact vertex is located on a different side of the equilibrium curve, i.e. the linear grasp is stable if the line intersects the equilibrium curve.
- if the contact situation is in the other area. The contact situation cannot be stable since either there is no equilibrium position for this quadrant (tendon-driven finger), or it is past the hyperflexion/hyperextension limit.

Then, it was assumed that the contact situations of both vertices stay in the same quadrant. Furthermore, one should note that only the extremity of the line physically in contact with a phalanx is to be taken into account. Obviously, if the line goes on beyond the phalanx, only the last point in contact with the latter has to be considered. Different cases are illustrated in Figs. 14 and 15:

- **(a)**: both vertices are stable, the grasp will be stable and contact will only remain with the (rightmost) second vertex;
- **(b)**: both vertices are unstable, the grasp will be unstable, opening-ejection occurs by crossing the hyperextension limit;
- **(c)**: first vertex is stable and the second is unstable, the grasp will be stable, contact with the whole line is maintained;
- **(d)**: first vertex is stable and the second is unstable, the latter is not physically on the phalanx, the grasp will be stable and contact with the line is maintained;
- **(e)**: first vertex is unstable and the second is stable, the grasp will be stable and contact will remain only with the stable vertex;
- **(f)**: first vertex is stable and the second is unstable, the grasp is unstable, closing-ejection will occur!

As it can be seen, a linear contact generally has a stabilizing effect on the grasp: configurations with an unstable vertex can be stable if the other vertex is so, except in the case where the first one belongs to a closing-ejection zone. This kind of ejection tends to destabilize the grasp, very similarly to the previous case: a stable vertex can be "destabilized" if the other vertex belongs to such a zone. Therefore, this kind of ejection seems to be particularly penalizing in terms of stability for the grasp and should be avoided.

4.3.2 Circular contact

In this case, the contact trajectories depend on the two parameters defining the circle, namely the position of the centre of the circle with respect to the base joint of the finger and the radius of the circle. One has:

$$k_2^2 + R_c^2 - d^2 + l_1^2 + 2l_1(k_2 \cos\theta_2 - R_c \sin\theta_2) = 0 \tag{16}$$

where d is the distance between the base joint of the finger and the centre of the circle, and R_c is its radius. Using an arbitrary initial contact state, the latter equation can be rewritten as:

$$k_2^2 - k_{2i}^2 + 2l_1(R_c(\sin\theta_{2i} - \sin\theta_2) + k_2 \cos\theta_2 - k_{2i} \cos\theta_{2i}) = 0 \tag{17}$$

where (k_{2i}, θ_{2i}) is the initial contact situation. Eq. (16) is a quartic in the plane (k_2,tan($\theta_2/2$)). One can draw the contact trajectories corresponding to a cylinder, illustrated by dotted lines in Fig. 16). In this plot, only the distance from the base joint is changed, and the radius of the circular object is constant. For each position of the object one obtains another trajectory. One should note that the smaller the radius, the more the contact trajectories tend to converge to the trajectories defined for a single point of contact. Mathematically, if $R_c = 0$ eq. (17) reduces to eq. (14). In Fig. 16, only the central quadrant is represented since it was established in the previous sections that no equilibrium is possible outside the latter. Studying the contact trajectories indicates that in the case of circular contact, the opening-ejection is usually minimized due to the slope of the contact trajectories (illustrated in Fig. 16). On the contrary, in the case of closing-ejection, the same slope of the curve actually increases the occurrence of ejection. Since cylindrical contact is more likely to happen than a single point contact, closing ejection is again particularly penalizing in terms of stability for the grasp.

4.3.3 Arbitrary contact shape

By studying every possible case of local curvature of the object, one can describe the behaviour of the finger grasping an arbitrary shaped-object which can be decomposed in sequential/continuous variation of these basic shapes. For instance varying the curvature will allow the study of an ovoid object while line and edge contacts can be used for a polygon. For example, a circular object partially cut is presented in Fig. 18 with its corresponding grasp-state plane equivalent. Note that the equilibrium curve does not appear since it depends on the transmission used and the latter does not influence the contact trajectory. If no theoretical results about an arbitrary shaped object can be given, practical considerations result from the previous analyses: *usually*, a single point of contact is the worst case that can happen in term of grasp stability, *except* when closing-ejection occurs. The latter noticeably increases unstable domains in the grasp-state plane for both linear and circular contact. The method to study the grasp stability of an underactuated two-phalanx finger has been presented for different cases of contact geometry leading to different grasp-state contact trajectories. Basically, it should be verified that this curve intersects either the equilibrium curve or the joint limit lines, this is a necessary but not sufficient condition for grasp stability. To obtain a decisive answer about the latter, the contact evolution direction on the trajectory should also be considered.

5 Conclusions

This paper has studied the grasp capability of two-phalanx underactuated fingers using a grasp-state technique. The aim of this paper is to acknowledge the impossibility for an underactuated finger to always apply forces on the object seized with both phalanges, hence to satisfy the criteria presented in [17] is impossible. If a situation where one phalanx force is negative occurs, one must study the motion undergone by the finger because the latter can lead either to a stable grasp, where this two-phalanx finger is fully constrained by only one contact, or to an ejection of the object. To ensure a stable grasp, ejection must be prevented. Contrary to previous studies [16], the paper has given the method to establish the equilibrium and trajectories in this grasp-state plane for *any* underactuated finger. Furthermore, a refined model considering friction, springs, and the local geometry of the object at the contact point are also contributions of the paper. The grasp-state representation presented in this work allows to predict the finger behaviour and ensure the grasp stability which has to be considered in designing underactuated fingers. The grasp-state plane can be extended to a grasp-state *space* for n-phalanx ($n > 2$) underactuated fingers. The case for $n = 3$ is of particular interest, especially with prosthetic applications, and is investigated in [20] where a three-dimensional grasp-state space is presented and discussed.

Acknowledgments

The financial support of Natural Sciences and Engineering Research Council of Canada (NSERC) and the Canada Research Chair Program is acknowledged.

References

[1] S. C. Jacobsen, E. K. Iversen, D. F. Knutti, R. T. Johnson, and K. B. Biggers. Design of the utah/mit dextrous hand. In *Proceedings of the 1986 IEEE International Conference on Robotics and Automation*, pages 1520–1532, San Francisco, CA, USA, 1986.

[2] J. K. Salisbury and J. J. Craig. Articulated hands: Force control and kinematic issues. *The International Journal of Robotics Research*, 1(1):4–17, 1982.

[3] G. A. Bekey, R. Tomovic, and I. Zeljkovic. *Control Architecture for the Belgrade/USC Hand in Dextrous Robot Hands.* Springer-Verlag, New-York, 1999.

[4] N. T. Ulrich. *Methods and Apparatus for Mechanically Intelligent Grasping*. US Patent No. 4 957 320, 1988.

[5] J. Butterfass, M. Grebenstein, H. Liu, and G. Hirzinger. Dlr-hand ii: Next generation of a dextrous robot hand. In *Proceedings of the 2001 IEEE International Conference on Robotics and Automation*, pages 109–114, Seoul, Korea, May 21-26 2001.

[6] T. Okada. Computer control of multijointed finger system for precise object-handling. *IEEE Transactions on Systems, Man and Cybernetics*, 12(3):289–299, 1982.

[7] A. Bicchi and V. Kumar. Robotic grasping and contact: A review. In *Proceedings of the IEEE International Conference on Robotics and Automation*, pages 348–353, San Francisco, CA, USA, 2000.

[8] M. Rakic. Multifingered robot hand with selfadaptability. *Robotics and Computer-integrated Manufacturing*, 3(2/3):269–276, 1989.

[9] S. Hirose and Y. Umetani. The development of soft gripper for the versatile robot hand. *Mechanism and Machine Theory*, 13:351–358, 1978.

[10] T. Laliberté and C. Gosselin. Simulation and design of underactuated mechanical hands. *Mechanism and Machine Theory*, 33(1/2):39–57, 1998.

[11] M. C. Carrozza, F. Vecchi, F. Sebastiani, G. Cappiello, S. Roccella, M. Zecca, R. Lazzarini, and P. Dario. Experimental analysis of an innovative prosthetic hand with proprioceptive sensors. In *Proceedings of the IEEE International Conference on Robotics and Automation*, pages 2230–2235, Taipei, Taiwan, 2003.

[12] M. Higashimori, M. Kaneko, A. Namiki, and M. Ishikawa. Design of the 100g capturing robot based on dynamic preshaping. *International Journal of Robotics Research*, 24(9):743–753, September 2005.

[13] H. Mochiyama, S. Hiramatsu, and Y. Mori. The frenet-serret manipulator. In *Proceedings of the IEEE/ASME International Conference on Advanced Intelligent Mechatronics*, pages 20–25, Como, Italy, July 2001.

[14] K. Salisbury. Whole arm manipulation. In *Proceedings of the 4th International Symposium on Robotics Research*, pages 183–189, Santa Cruz, California, USA, August 9-14 1987.

[15] P. D. Panagiotopoulos and A. M. Al-Fahed. Robot hand grasping and related problems: Optimal control and identification. *International Journal of Robotics Research*, 13(2):127–136, April 1994.

[16] L. Birglen and C. Gosselin. On the force capabilities of underactuated fingers. In *Proceedings of the 2003 IEEE International Conference on Robotics and Automation*, pages 1139–1145, Taipei, Taiwan, September 2003.

[17] L. Birglen and C. Gosselin. Kinetostatic analysis of underactuated fingers. *IEEE Transactions on Robotics and Automation*, 20(2):211–221, April 2004.

[18] L. Birglen. *Analysis and Control of Underactuated Robotic Hands*. PhD thesis, Faculté des sciences et de génie, Université Laval, Québec, Canada, October 2004.

[19] M. Kaneko and T. Hayashi. Standing-up characteristic of contact force during self-posture changing motions. In *Proceedings of the IEEE International Conference on Robotics and Automation*, pages 202–208, 1993.

[20] L. Birglen and C. M. Gosselin. Geometric design of three-phalanx underactuated fingers. *ASME Journal of Mechanical Design, in press*, March 2006.

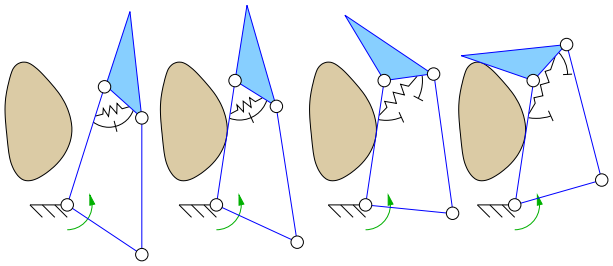

Fig. 1. Closing sequence of a 2-phalanx finger with linkage transmission.

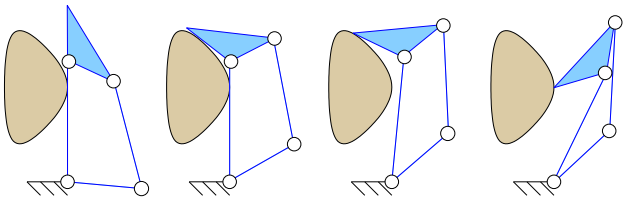

Fig. 2. Example of an ejection sequence.

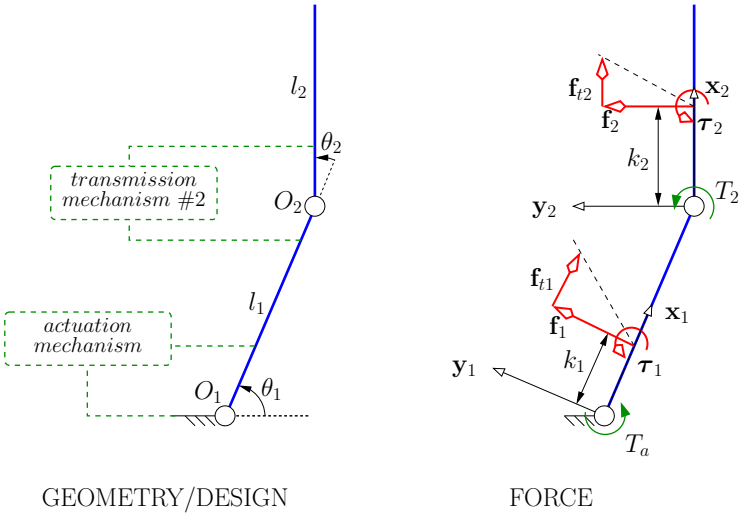

Fig. 3. Conceptual two-phalanx underactuated finger.

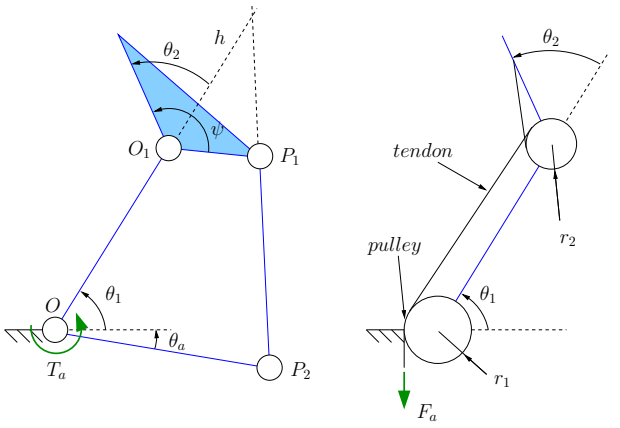

Fig. 4. Common transmission: mechanical linkage and pulley-tendon.

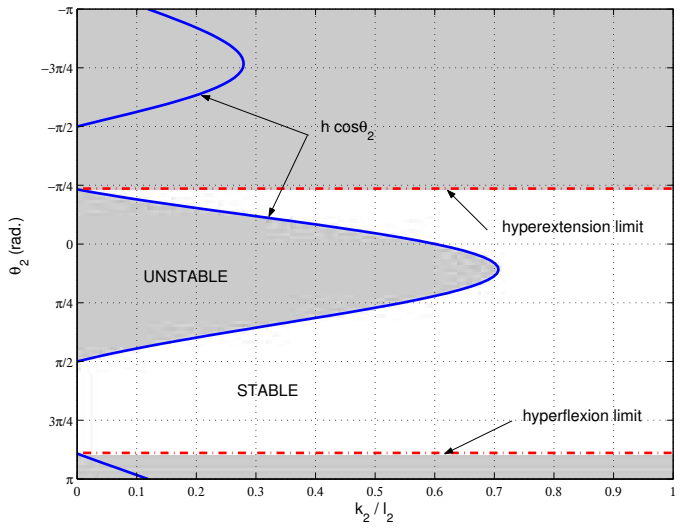

Fig. 5. Grasp-state plane: positive zones for $\mathbf{f}$ (parameter set 1).

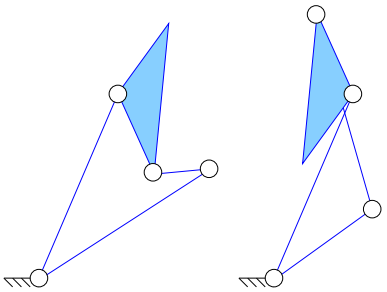

Fig. 6. Hyperextension/hyperflexion configurations.

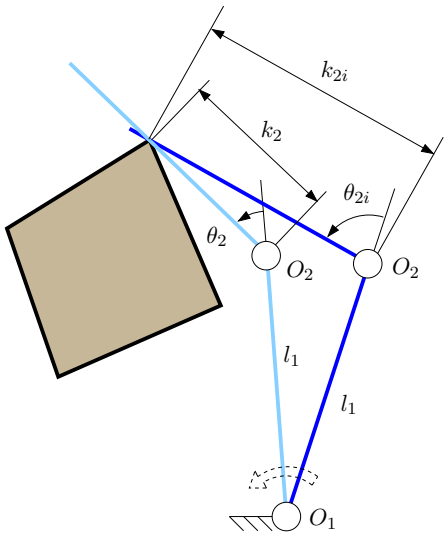

Fig. 7. Grasp-state illustration.

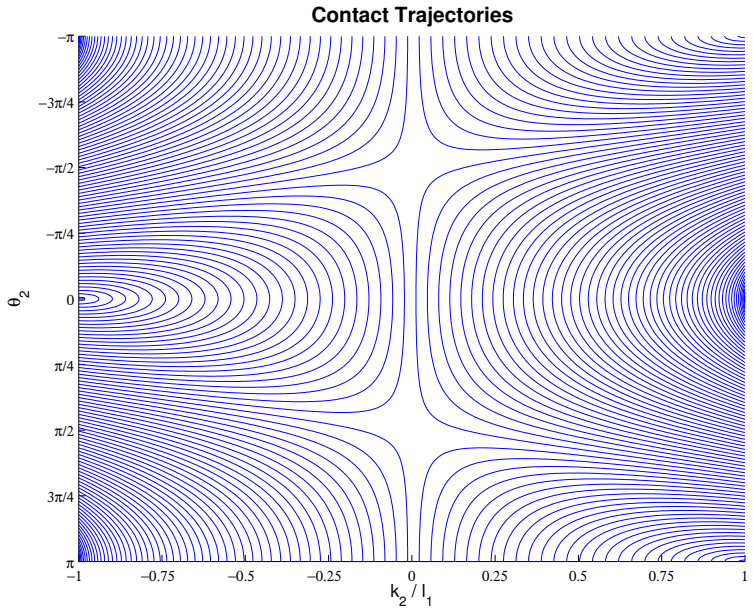

Fig. 8. Contact trajectories in (k_2,θ_2).

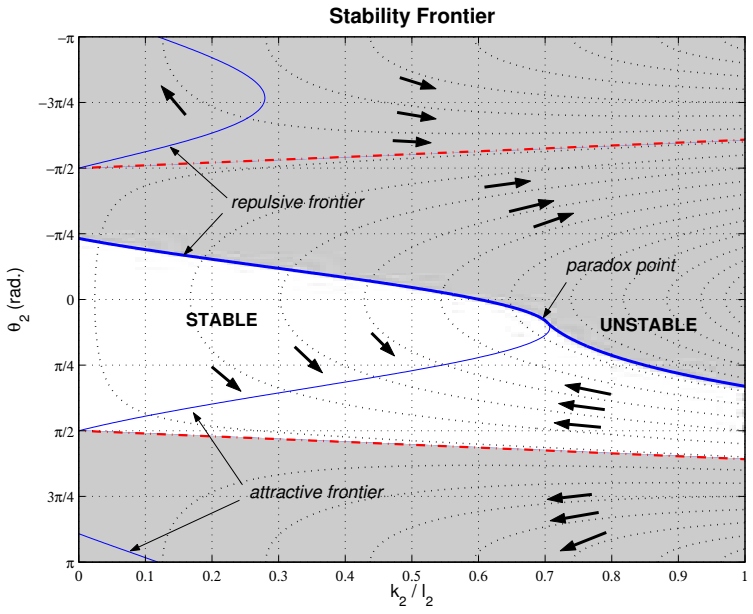

Fig. 9. Final stability of the grasp with one phalanx contact — parameter set 1

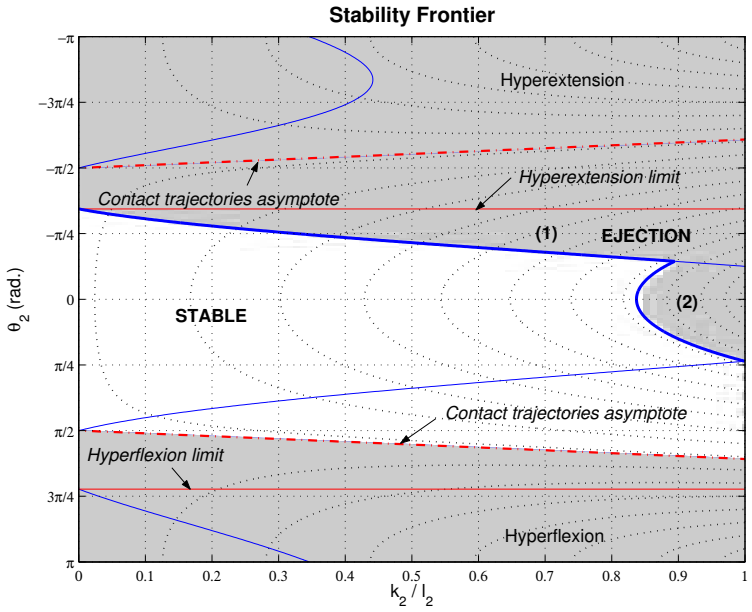

Fig. 10. Final stability of the grasp with one phalanx contact — parameter set 2

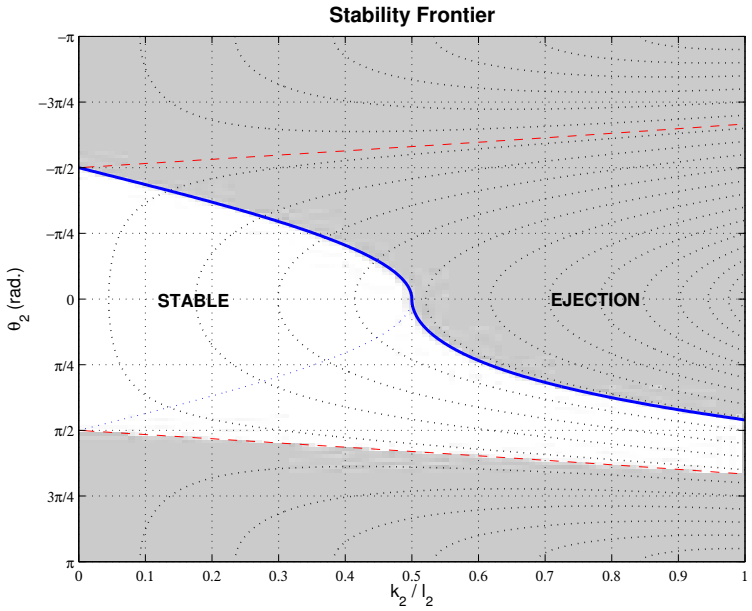

Fig. 11. Final stability of the grasp with one phalanx contact — Soft Gripper

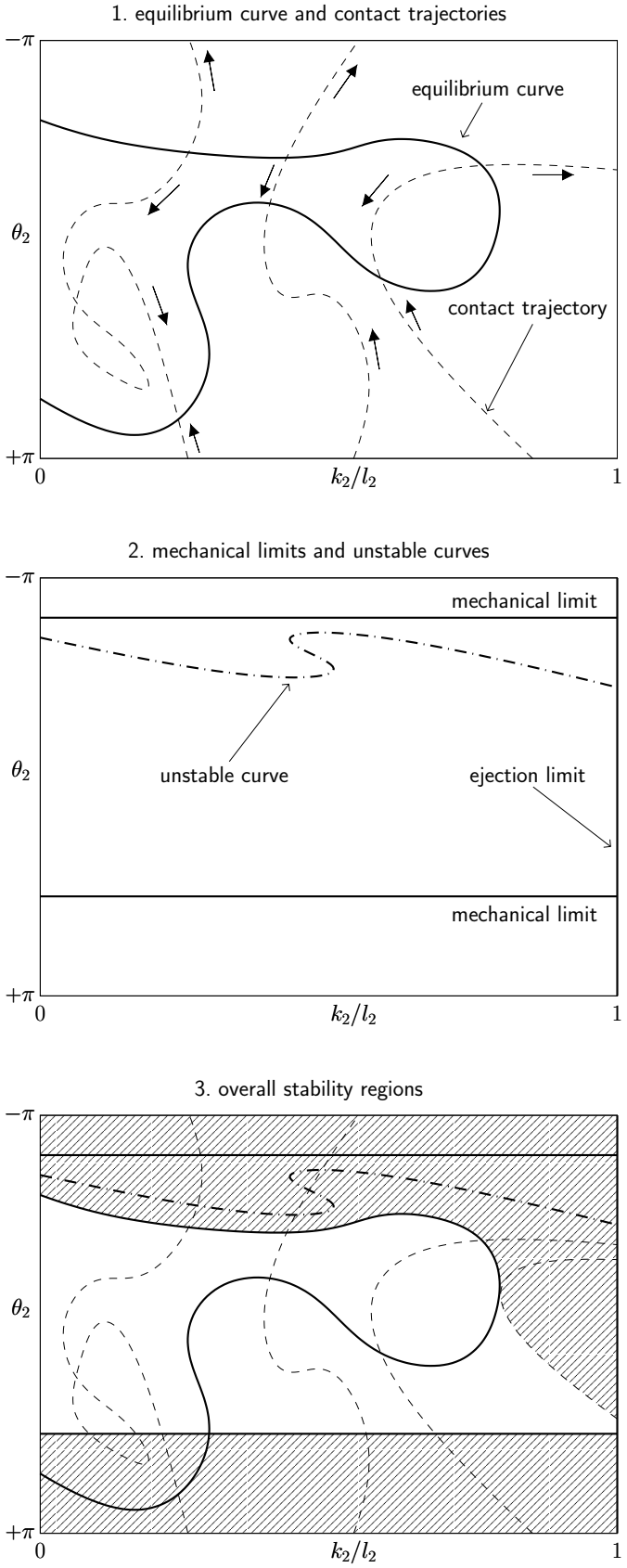

Fig. 12. Construction of the stability regions

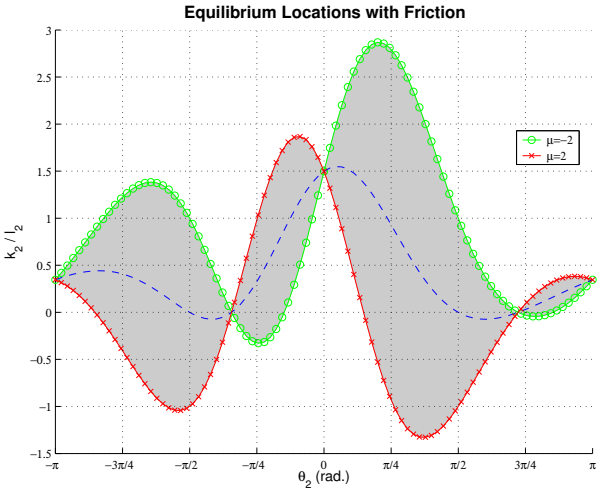

Fig. 13. Stable areas with friction (parameter set 2).

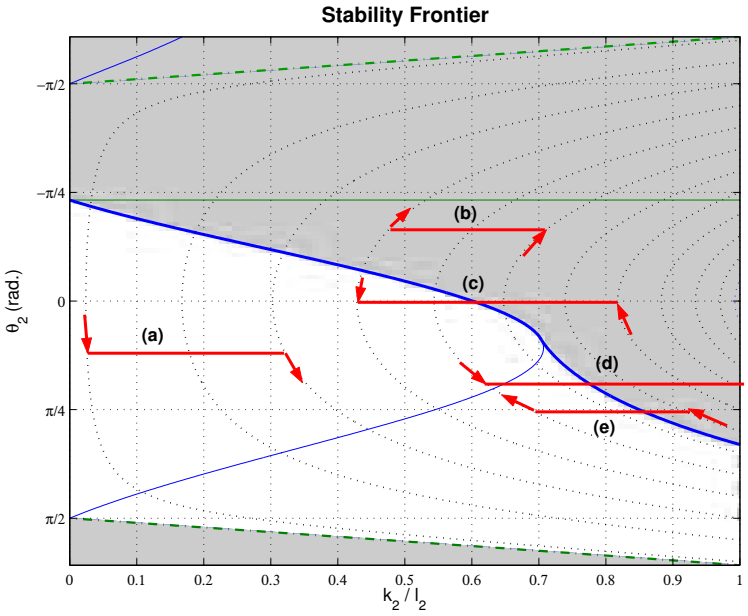

Fig. 14. Linear contact stability (parameter set 1).

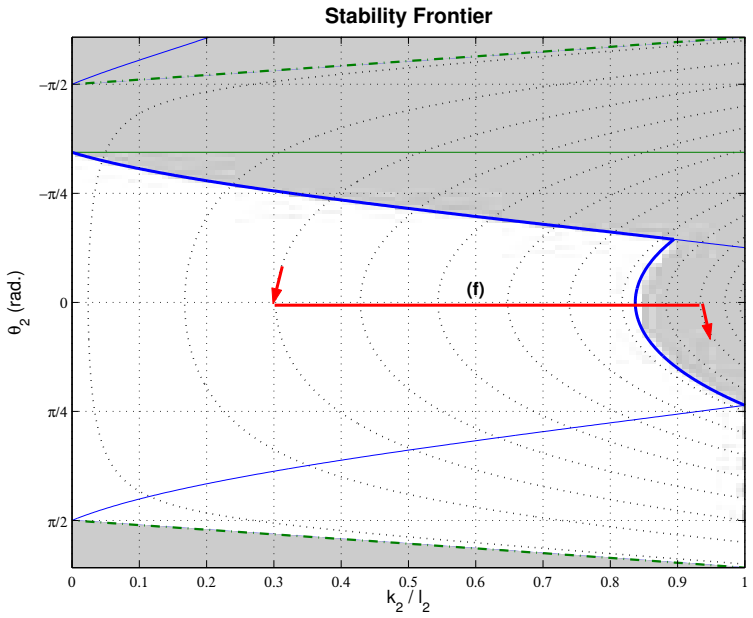

Fig. 15. Linear contact stability (parameter set 2).

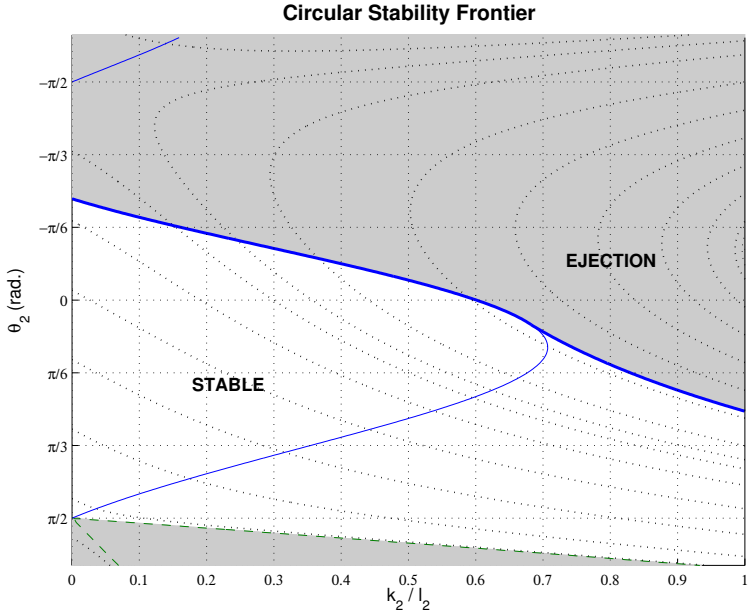

Fig. 16. Stability of the grasp with one phalanx cylindrical contact (parameter set 1, $R_c = l_1/4$).

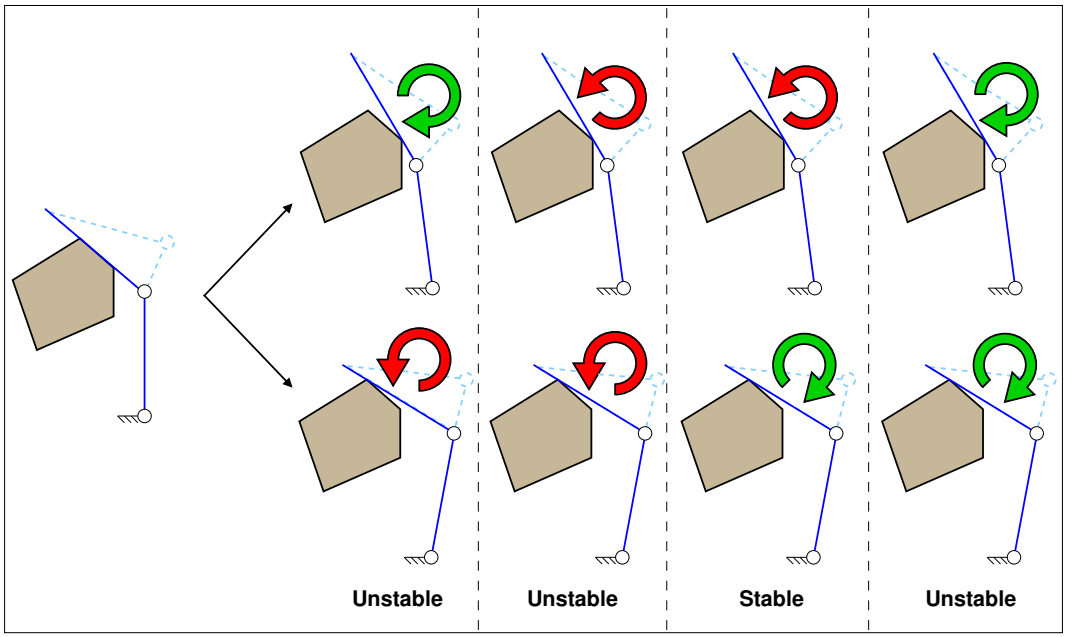

Fig. 17. Stability of the initial linear contact

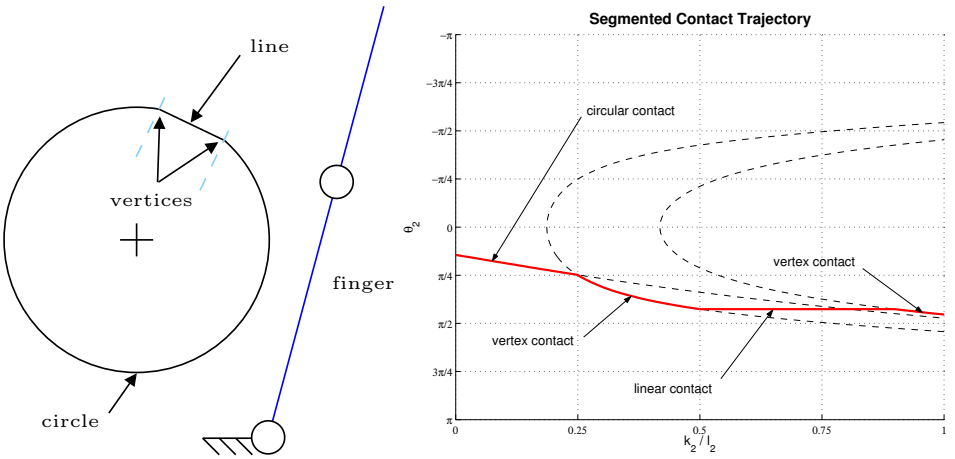

(a) Cartesian plane (b) Grasp-state plane

Fig. 18. Segmentation example.